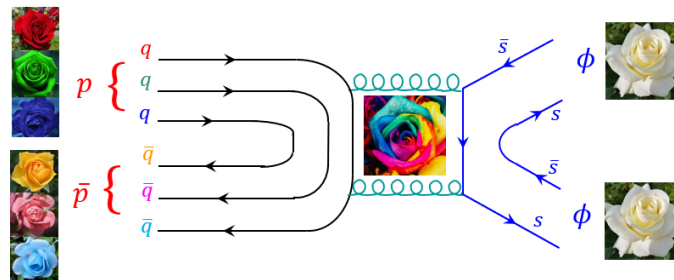


*Proposal for J-PARC 50 GeV Proton Synchrotron*  
**Double  $\phi$  Production in  $\bar{p}p$  Reactions near Threshold**




---

Spokesperson	Jung Keun Ahn (Korea University)
Beam line	K1.8BR
Beam	$\bar{p}$ / 0.90–1.15 GeV/c in 0.05 GeV/c increments
Beam Intensity	$2.7 \times 10^5$ / spill (4.24 s spill duration)
Target	Liquid hydrogen (80 mm $\phi$ )
Reaction	$\bar{p}p \rightarrow \phi\phi$
Detector	Hyperon Spectrometer (HypTPC)
Beam time	6.5 days (0.5 days for trigger study and 6 days for physics runs)
Expected yield	$3 \times 10^3$ events

---

July 1, 2024

# The $\phi\phi$ Collaboration

J.K. Ahn (*Spokesperson*), B.M. Kang, W.S. Jung, Y.J. Kim, H.I. Lee  
*Korea University, Seoul, Korea*

T. Ishikawa, S.Y. Ryu, K. Suzuki, K. Mizutani, A. Higashi  
*RCNP, Osaka University, Osaka, Japan*

H. Ohnishi  
*RARIS, Tohoku University, Sendai, Japan*

F. Sakuma, Y. Ma, T. Hashimoto  
*RIKEN, Wako, Japan*

T. Takahashi  
*KEK, Ibaraki, Japan*

S.i. Nam, D.Y. Lee  
*Pukyong National University, Korea*

I. Strakovsky  
*The George Washington University, US*

Y. Ichikawa, S.H. Hayakawa, F. Oura, R.J. Saito, K. Amemiya, K. Shimazaki  
*Department of Physics, Tohoku University, Japan*

K. Tanida, H. Sako, S. Sato, T.O. Yamamoto  
*ASRC, Japan Atomic Energy Agency, Japan*

S.H. Kim  
*Kyungpook National University, Korea*

N. Tomida, R. Koike  
*Kyoto University, Japan*

## Abstract

The purpose of the experiment is to investigate rare aspects of the reaction  $\bar{p}p \rightarrow \phi\phi$  in hitherto unexplored energy region close to threshold. with HypTPC..We propose a new experiment to study double  $\phi$  production in  $\bar{p}p$  reactions in the momentum range of 0.90 ( $\sqrt{s} = 2.05$ ) to 1.15 GeV/c ( $\sqrt{s} = 2.13$  GeV) at the K1.8BR beam line. The cross section near the threshold, reported by the JETSET collaboration, shows an unusually high violation of the OZI rule in the  $\bar{p}p \rightarrow \phi\phi$  reaction. This violation, a few mb, is two orders of magnitude higher than the expected value of 10 nb from the SU(3) flavor mixing.

The proposed experiment will provide the first-ever data from threshold to 1.1 GeV/c, a region that has never been explored. The experiment aims to collect enough event statistics to measure the polarization observables in high momentum settings. These observables include spin density matrix elements and spin correlation variables.

A large acceptance of the HypTPC enables the measurement of the  $\bar{p}p \rightarrow \phi\phi$  reaction. This experiment should be conducted following the E72 during stable HypTPC operation. We are requesting 6.5 days of beam time, which includes half a day for the trigger study.

This experiment can be classified as a test experiment and it could also be a part of the experiment E29, which is focused on searching for  $\phi$  meson bound state by H. Ohnishi, The cross section of the elementary process  $\bar{p}p \rightarrow \phi\phi$  provides important information for studying  $\phi N$  interaction in both free space and a nuclear medium. The proposed experiment will also yield significant information on the double strangeness production of nuclear cluster states with a helium target (Double  $K^-$  production in nuclei by stopped  $\bar{p}$  annihilation by F. Sakuma).

# 1 Introduction

The proposed experiment will focus on studying the annihilation of  $\bar{p}p$  into  $\phi\phi$  from just above the threshold of 0.90 GeV/c up to 1.15 GeV/c. This reaction  $\bar{p}p \rightarrow \phi\phi$  provides an excellent opportunity to investigate the dynamics of gluons in hadrons. In a simple model, all  $q\bar{q}$  pairs of the initial  $\bar{p}p$  state give rise to two  $s\bar{s}$  pairs.

Despite the OZI suppression, the JETSET experiment[1] reported cross sections on the order of a few  $\mu\text{b}$ , which is two orders of magnitude higher than what was predicted by the  $\omega$ - $\phi$  mixing. Moreover, there are no experimental data available from the threshold to 2.15 GeV, where the baryon exchange amplitude could potentially have an effect.

We aim to tackle the critical issue of understanding the dynamics of gluons by conducting a comprehensive investigation of the interaction between the meson and nucleon, which do not have the same flavor of quarks and are restricted from exchanging quarks in a single step. The  $\bar{p}p \rightarrow \phi\phi$  is the most suitable reaction for this study.

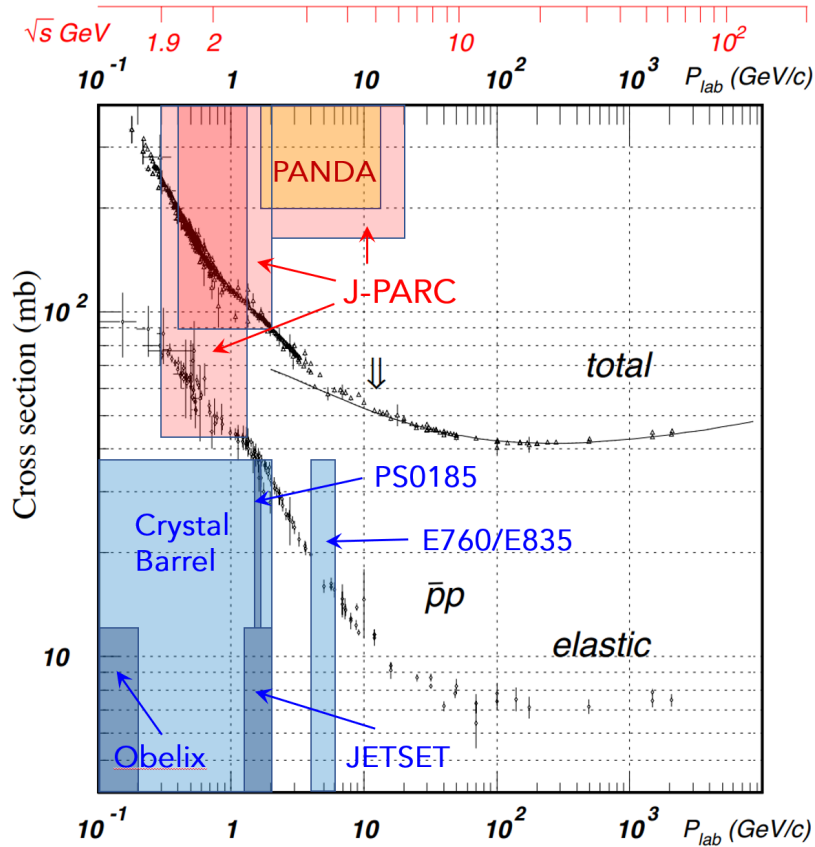


Figure 1: The cross sections for  $\bar{p}p$  reactions are described as functions of beam momentum and center-of-mass energy. The blue boxes represent the beam momentum ranges covered by old experiments, while the red boxes depict the range covered by the current J-PARC beam lines and the future PANDA detector at HESR.

Antiproton beams are currently available only at J-PARC. The High Energy Storage Ring (HESR) of GSI is designed to produce high-intensity antiproton beams with energies above  $\sqrt{s} = 2.25$  GeV ( $p = 1.5$  GeV/c). These beams collide with the fixed target inside the PANDA detector at GSI, but the facility's operation is still pending. J-PARC can supply antiproton beams at K1.8BR, K1.8 and high-p beam lines, each covering different energy ranges illustrated in Fig. 1. The K1.8BR beam line, with a maximum beam momentum of 1.2 GeV/c, is suitable for the  $\bar{p}p \rightarrow \phi\phi$  reaction. This reaction specifically requires the low beam momentum offered by this beam line, since reactions involving additional pions necessitate higher beam momenta.

Table 1 displays the threshold laboratory momentum for each reaction involving  $\phi\phi$  in the final state with different beam particles. For the formation of a  $\phi\phi$  state, other hadron and photon beams must have momenta exceeding 4 GeV/c.

$\phi\phi$ Production Reactions	$p_{\text{thre}}^{\text{lab}}$ (GeV/c)
$\bar{p}p \rightarrow \phi\phi$	0.866
$\bar{p}p \rightarrow \phi\phi\pi^0$	1.285
$\bar{p}p \rightarrow \phi\phi\pi^+\pi^-$	1.681
$\pi^-p \rightarrow \phi\phi n$	4.246
$\gamma p \rightarrow \phi\phi p$	4.254
$K^-p \rightarrow \phi\phi\Lambda$	4.677

Table 1: Threshold momenta for  $\phi\phi$  production in various reactions and background processes with four charged particle emission.

The decay of  $\phi$  into  $K^+K^-$  is detected in this process using the HypTPC. This proposed experiment will follow experiment E72, allowing for a smooth transition to the  $\bar{p}p$  experiment by changing only beam line parameters. This experiment can be considered a test experiment named "T", and it could also be a part of the experiment E29 (Searching for  $\phi$  meson bound state by H. Ohnishi [2]). The cross section of the elementary process  $\bar{p}p \rightarrow \phi\phi$  provides significant information for studying  $\phi N$  interaction in both free space and a nuclear medium. The proposed experiment will also yield important information on the double strangeness production of nuclear cluster states with a helium target (Double  $K^-$  production in nuclei by stopped  $\bar{p}$  annihilation by F. Sakuma) [3].

The experiment can also investigate other reactions such as  $\omega\phi$  and  $\bar{K}^{*0}K^{*0}$ , where  $\omega \rightarrow \pi^0\pi^+\pi^-$  and  $K^{*0} \rightarrow \pi^-K^+$ . This proposal will review theoretical predictions and previous experimental results in Section 2. Detailed information about the experiment is provided in the following section. The beam time request is summarized in Section 4, and the current status of the experiment and costs are briefly discussed in Section 5. Section 6 summarizes the experimental proposal.

## 2 Physics Motivation

### 2.1 Production Mechanisms

According to the naive constituent quark model, the proton (antiproton) wave function contains only up and down quarks (antiquarks), whereas the  $\phi$  meson is nearly a pure  $\bar{s}s$  state. Consequently, the reaction  $\bar{p}p \rightarrow \phi\phi$  may occur through two gluon emission from the  $\bar{q}q$  annihilation, as depicted in Fig. 2(a). All three valence quarks in the proton annihilate with the corresponding three antiquarks in the antiproton to create a purely gluonic state, from which  $\phi\phi$  is formed. According to the Okubo-Zweig-Iizuka (OZI) rule, this process, with its disconnected quark lines, should be strongly suppressed.

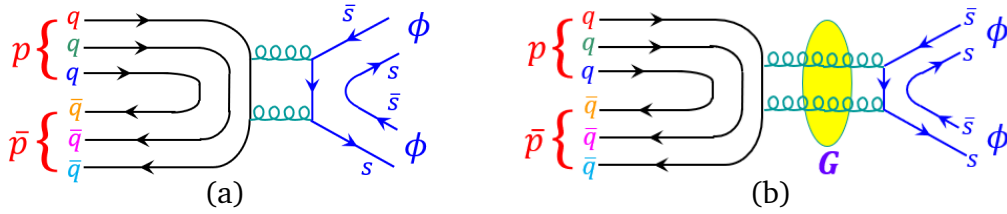


Figure 2: (a) Quark line diagram for  $\bar{p}p \rightarrow \phi\phi$  reaction via two gluon emission and (b) a resonant gluonic state called a glueball.

However, the JETSET collaboration has seen unusually highly apparent violation of the OZI rule in the  $\bar{p}p \rightarrow \phi\phi$  reaction [1]. The measured cross section of this reaction turns out to be 2–4  $\mu\text{b}$  for momenta of incoming antiprotons from 1.1 to 2.0 GeV/c. It is two orders of magnitude higher than the value of 10 nb which is expected from the OZI rule.

A substantial OZI rule violation could be the signal of interesting new physics. There are several intriguing possibilities that lead to large  $\phi\phi$  production cross section: (1) production of glueballs, (2) coupling to broad four quark states involving  $\bar{s}s$  such as  $\phi(2170)$ [4] and  $X(2239)$ [5], (3) the non-strange quark component of the  $\phi$  meson, due to the actual mixing of the vector meson singlet and octet, (4) the presence of substantial  $\bar{s}s$  content in  $\bar{p}p$  wave functions, (5) the instanton induced interactions between quarks, (6) the hadron loops in which each individual transition is OZI-allowed, and (7) the baryon exchange in  $t$ - and  $u$ - channel diagrams.

The large OZI violation can occur if a resonant gluonic state such as a glueball or a four quark state containing a sizable  $\bar{s}s$  admixture contributes to the  $\bar{p}p \rightarrow \phi\phi$  reaction. Since gluons are spin 1 massless particles, possible spin-parity states are  $J^{PC} = 0^{++}, 0^{-+}, 2^{++}$  for 2 gluons ( $J = 0$  or  $2, P = (-1)^{L+1} = \pm 1$ , and  $C = (-1)^{L+S} = \pm 1$ ). Lattice QCD results predict the masses of the  $2^{++}$  and  $0^{-+}$  glueballs to be well above 2 GeV, around  $(2.39 \pm 0.12)$  and  $(2.56 \pm 0.12)$  GeV[6]. However, some phenomenological model calculations point to the mass region near 2.0 GeV, which can be accessed by near-threshold  $\phi\phi$  production experiments. A theoretical study using QCD sum rules suggests that the masses of the  $2^{++}$

and  $0^{-+}$  glueballs are estimated to be  $(2.0 \pm 0.1)$  and  $(2.05 \pm 0.19)$  GeV, respectively [7]. In contrast, a recent QCD sum rule calculation predicts the masses of the  $2^{++}$  and  $0^{-+}$  glueballs are  $(1.86 \pm 0.17)$  and  $(2.17 \pm 0.11)$  GeV [8].

Alternatively, the reaction  $\bar{p}p \rightarrow \phi\phi$  may occur through a two-step process involving meson pairs, such as  $\omega\omega$ . The  $\omega\omega$  could be directly produced from the  $\bar{p}p$  initial state, with  $\omega$ - $\phi$  mixing resulting in the creation of the  $\phi\phi$  state. Due to a slight discrepancy from the ideal mixing of the vector meson singlet and octet, an upper limit for the total cross section of the  $\bar{p}p \rightarrow \phi\phi$  can be determined relative to the total cross section of the  $\bar{p}p \rightarrow \omega\omega$ . This can be expressed as:

$$\sigma(\bar{p}p \rightarrow \phi\phi) = \tan^4 \delta \cdot \sigma(\bar{p}p \rightarrow \omega\omega) \approx 10 \text{ nb.}$$

This approximation holds true if both  $\phi$ 's were produced by independent OZI-violating couplings. In this context, the angle  $\delta(= \Theta_i - \Theta)$  denotes the difference between the ideal mixing angle  $\Theta_i = 35.3^\circ$  ( $\sin \Theta_i = 1/\sqrt{3}$ ) and the mixing angle  $\Theta$  between  $(\phi, \omega)$  mesons and the SU(3) states  $(\omega_0, \omega_8)$ .

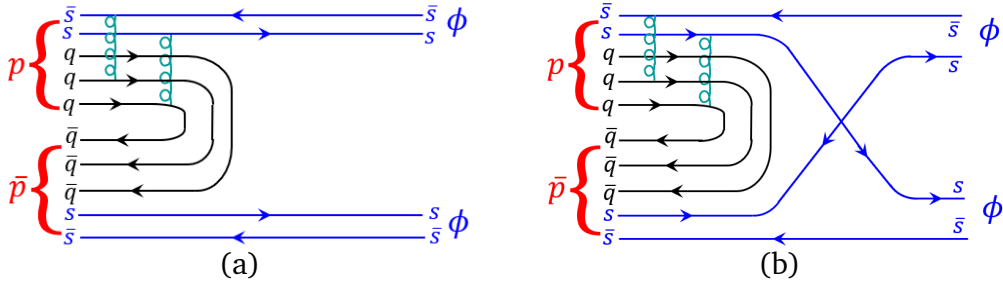


Figure 3: Quark line diagrams for  $\bar{p}p \rightarrow \phi\phi$  reaction via (a) a shake-out and (b) rearrangement process with strangeness content of the proton and antiproton.

One interesting possibility is that strange quarks could be knocked off directly from the  $\bar{q}q$  sea of the proton and the antiproton to form a pair of  $\phi$  mesons:  $\phi\phi$ . Strangeness content ( $^1S_0 \bar{s}s$ ) of the proton and antiproton might lead to the production of  $\phi\phi$  through a shake-out or rearrangement process[9] as depicted in Fig. 3(a) and (b). Importantly, this process does not violate the OZI rule because it involves connected quark diagrams with higher Fock-space components in the nucleon wave function:

$$|p\rangle = x \sum_{X=0}^{\infty} |uudX\rangle + z \sum_{X=0}^{\infty} |uud\bar{s}sX\rangle, \quad |x|^2 + |z|^2 = 1,$$

where  $X$  stands for any number of glueons and light  $\bar{q}q$  pairs. The upper limit for the total

cross section of the  $\bar{p}p \rightarrow \phi\phi$  reaction is given by

$$\sigma(\bar{p}p \rightarrow \phi\phi) = \frac{|z|^4}{|x|^4} \cdot \sigma(\bar{p}p \rightarrow \omega\omega) \geq 250 \text{ nb},$$

which is larger than the value from the  $\phi$ - $\omega$  mixing effect, but still much smaller compared to the experimental data.

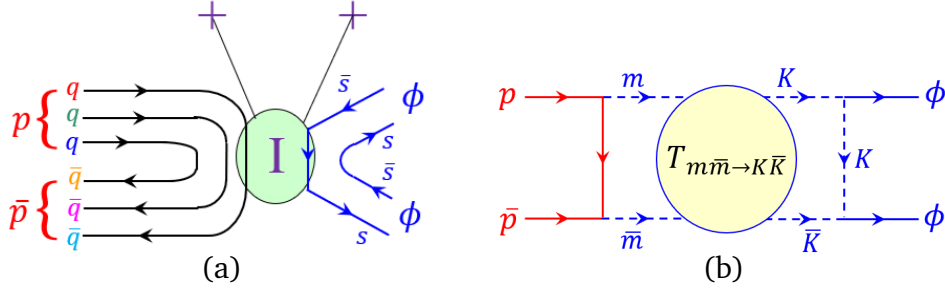


Figure 4: (a) Contribution of the instantons to the reaction  $\bar{p}p \rightarrow \phi\phi$ . The instanton is denoted as  $I$  and crosses mark the quark legs which are connected through vacuum and (b) rescattering diagram for  $\bar{p}p \rightarrow \phi\phi$ , involving the  $\bar{m}m \rightarrow \bar{K}K$  loops.

The interaction between quarks, induced by instantons, could potentially weaken the OZI suppression. A theoretical study[10] demonstrates that the violation of the OZI rule in the  $\bar{p}p$  annihilation is a nontrivial consequence of the complex structure of the QCD vacuum, which is associated with existence of the instantons, as depicted in Fig. 4(a).

On the other hand, the large cross section for the  $\bar{p}p \rightarrow \phi\phi$  reaction may be explained by considering the hadronic loop mechanisms. Each transition in the loop is OZI-allowed, as shown in Fig. 4(b). Lu *et al.* studied the role of a  $\bar{K}K$  intermediate state in a triangle diagram in the  $\bar{p}p \rightarrow \phi\phi$  reaction [11]. The intermediate  $\eta\eta$  can also contribute to the  $\phi\phi$  production, as the  $\eta$  contains  $\bar{s}s$  content. In addition, the  $\pi\pi \rightarrow \bar{K}K$  amplitude could make a sizable contribution. It is worth noting that the loop kernel  $\bar{B}B \rightarrow \bar{m}m$  involving a baryon and antibaryon pair is possible. A full calculation involving all possible hadronic loops would be necessary to predict the detailed shape and magnitude of the observed spectrum.

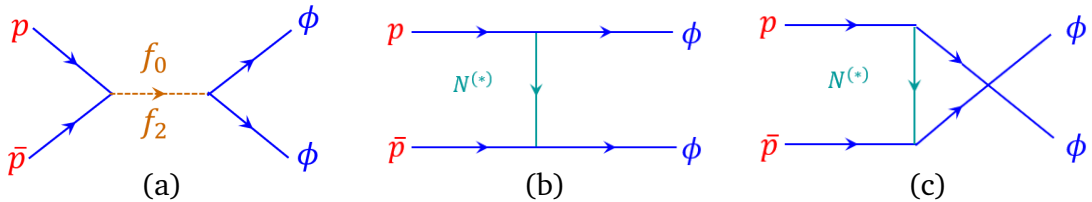


Figure 5: Relevant Feynman diagrams illustrate the (a)  $s$ -channel, (b)  $t$ -channel, and (c)  $u$ -channel amplitudes for  $\bar{p}p \rightarrow \phi\phi$ .



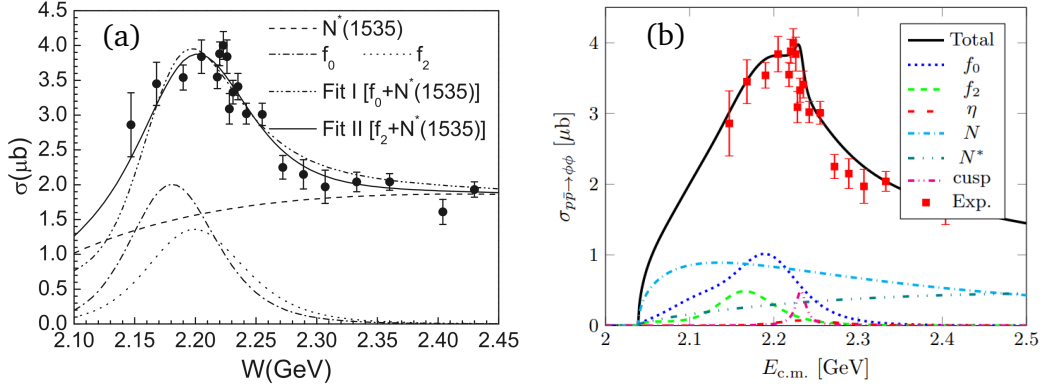


Figure 6: (a) Total cross-sections for  $\bar{p}p \rightarrow \phi\phi$  overlaid with theoretical calculation results for an  $N(1535)$  exchange with a  $f_0$  or  $f_2$  contribution, and (b) new theoretical calculation results involving  $N$  and  $N^*$  exchanges with all possible  $f_0$ ,  $f_2$ , and  $\eta$  contributions.

In the context of hadronic degrees of freedom, the  $\bar{p}p \rightarrow \phi\phi$  reaction can be described in terms of the meson and baryon exchange diagrams, as shown in Fig. 5. Recent theoretical calculations suggest that the  $N^*(1535)$  exchange in the  $t$ -channel could play a significant role and provide an important source for bypassing the OZI rule[12]. Additionally, a more recent theoretical calculation, using an effective Lagrangian approach, indicates that the inclusion of either  $f_0$  or  $f_2$  in the  $s$ -channel can effectively describe the bump structure near  $W \approx 2.2$  GeV[13]. These two previous work included only the  $N^*(1535)$  exchange. Fig. 6(a) shows total cross sections for the  $\bar{p}p \rightarrow \phi\phi$  reaction, overlaid with the contributions from  $s$ -channel  $f_0$  and  $f_2$ ,  $t$ - and  $u$ -channel  $N^*(1535)$  resonances.

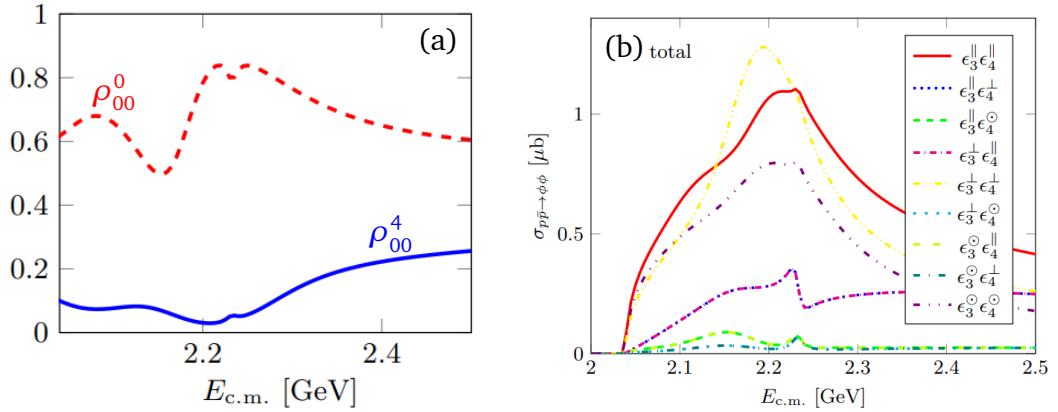


Figure 7: (a) Spin density matrix elements  $\rho_{00}^4$  and  $\rho_{00}^0$  for a  $\phi$  meson at  $\theta = 0$  and (b) spin correlations between two  $\phi$  mesons.

In a new theoretical study using an effective Lagrangian approach, the exchange of a ground state  $N$  and three  $N^*$  resonances with  $J^P = 1/2^-$  in the  $t$ - and  $u$ -channels ( $N^*(1650)$ ,  $N^*(1895)$ , and  $N^*(1535)$  in order of coupling strength) as well as all  $f_0$  and

$f_2$  mesons in the  $s$ -channel, are considered[14]. A theoretical work in a coupled-channel formalism shows that the  $N^*(1650)$  contributes to  $\phi N$  channel more significantly than in  $N^*(1535)$  [15], which indicates the previous work with only the  $N^*(1535)$  exchange may be insufficient. Additionally, a pseudoscalar meson,  $\eta(2225)$ , is added in the  $s$ -channel. In Fig. 6(b), the fit results are shown overlaid with various amplitude contributions. This study suggests that a measurement of spin observables such as spin density matrix elements  $\rho_{00}^0$  and  $\rho_{00}^4$  may offer a way to investigate individual amplitude contributions, as depicted in Fig. 7(a).

The spin-parity of a potential intermediate state can be constrained by examining the angular distributions of the  $\phi \rightarrow K^+K^-$  decay, particularly, the polar angle of the kaon in the rest frame of its parent  $\phi$  ( $\cos \theta_K$ ). The distribution of  $\cos \theta_K$  provides the spin direction of the  $\phi$ , allowing six independent spin correlations with a longitudinal and two transverse polarizations on the  $\phi\phi$  production plane, as shown in Fig. 7(b).

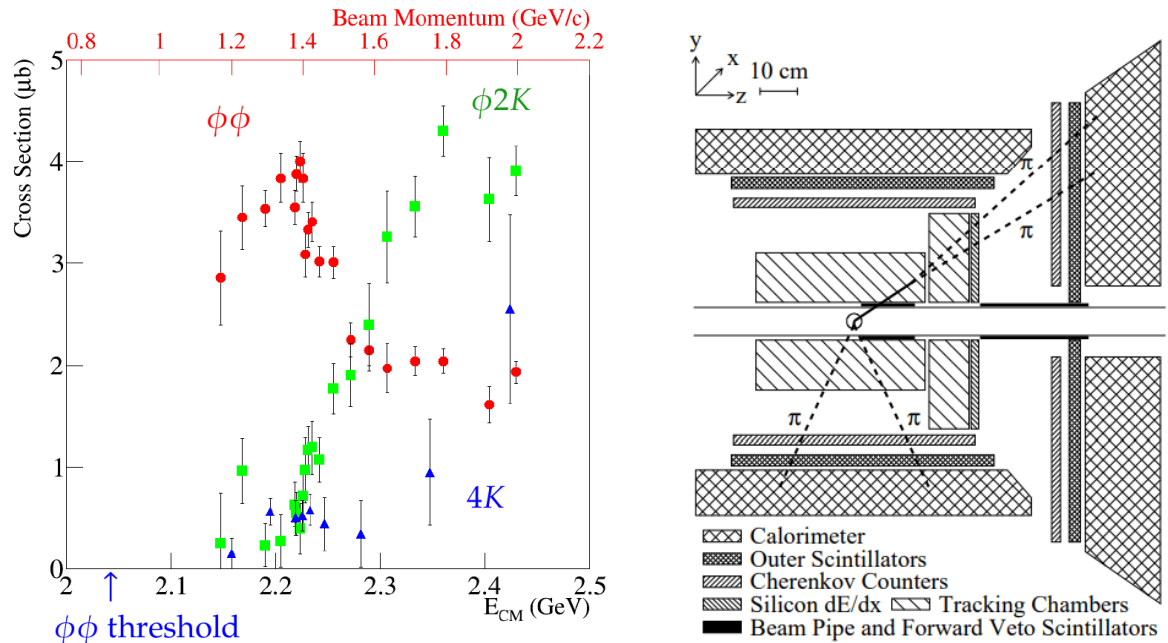


Figure 8: (a) Cross sections for  $\bar{p}p \rightarrow \phi\phi$ ,  $\phi 2K$ , and  $4K$  reactions measured by JETSET and (b) the cross-sectional view of the JETSET experiment.

## 2.2 Previous $\phi\phi$ Data

In three previous experiments, the production of  $\phi\phi$  in  $\bar{p}p$  annihilation was measured. The first report[16] was based on one  $\phi\phi$  event out of six  $2K^+2K^-$  events recorded in an ANL bubble chamber in the momentum range from 1.6 to 2.2 GeV/c. The estimated  $\phi\phi$  production was about 600 nb. At a center-of-mass energy of 3 GeV (approximately 3.7

GeV/c), the experiment R704 at CERN-ISR measured the cross section for  $\bar{p}p \rightarrow \phi\phi$  to be 25 nb[17]. The JETSET Collaboration at LEAR, CERN made the most recent measurement, where they observed an unexpectedly large magnitude for the  $\bar{p}p \rightarrow \phi\phi$  cross-section[1].

A spin-parity analysis of the  $\phi\phi$  system indicates that the  $J^{PC} = 2^{++}$  waves give the dominant contribution near the threshold [18]. Fig. 8 displays a layout of the JETSET/PS202 experiment, which shows the major detector components. A typical event with three forward and one barrel track is overlaid. The JETSET apparatus had no magnetic field, leading to the absence of charge information. The selected  $\bar{p}p \rightarrow 4K$  event candidates are illustrated in Fig. 9(a). Selecting one  $\phi$ , requiring one  $m(K_3K_4)$  combination to lie in the region 1.00–1.04 GeV/c<sup>2</sup>, the opposite combination  $m(K_1K_2)$  is shown in Fig. 9(b), where a clean  $\phi$  peak is visible.

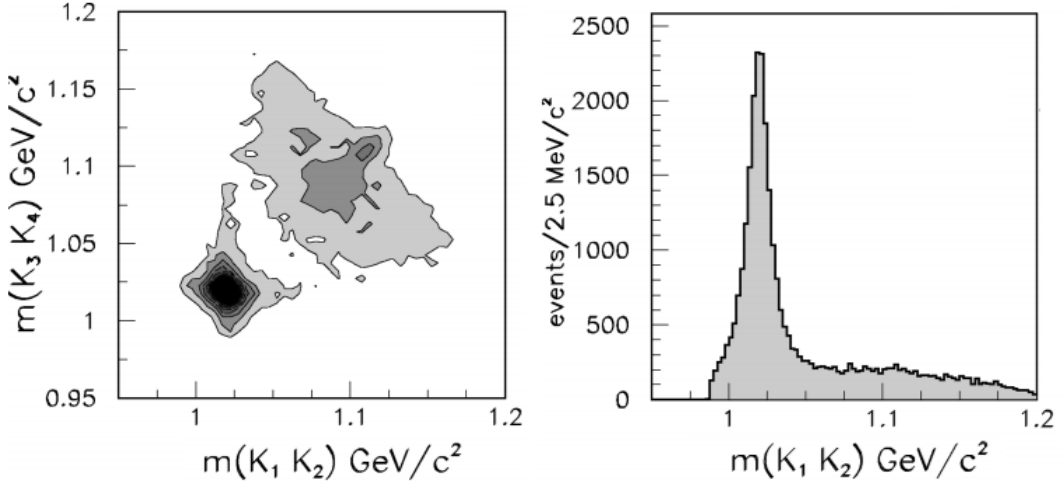


Figure 9: (a) Scatter plot of the  $KK$  invariant masses (three combinations per event because of the absence of charge information) and (b)  $K_1K_2$  mass projection for  $1.00 \geq M(K_3K_4) \geq 1.04$  GeV/c<sup>2</sup>.

In four separate experiments[19, 20, 21, 22] at BNL-AGS, the OZI forbidden reaction  $\pi^-p \rightarrow \phi\phi n$  was observed at a momentum of 22 GeV/c and the observed statistics increased. An excess of  $\phi\phi$  events was observed, surpassing the prediction, which indicated a potential violation of the OZI suppression. A partial-wave analysis revealed the presence of three  $2^{++}$  mesons. Furthermore, the experiment WA67 at the CERN-SPS investigated the inclusive reaction  $\pi^-Be \rightarrow \phi\phi + X$  and observed a  $\phi\phi$  mass spectrum with two broad  $2^{++}$  resonances.

It has been reported that the MARK III experiment at SLAC-SPEAR found a  $J^P = 0^-$  structure near the threshold in the  $\phi\phi$  mass spectrum for  $J/\psi \rightarrow \gamma\phi\phi$  decays[23]. Recently, BESIII observed  $4.6 \times 10^4$   $J/\psi \rightarrow \gamma\phi\phi$  events in the  $\phi\phi$  mass region below 2.7 GeV/c<sup>2</sup> out of a sample of  $1.3 \times 10^9$   $J/\psi$  events. The partial-wave analysis revealed that the observed structures were mainly  $0^{-+}$  states involving  $\eta(2100)$ ,  $\eta(2225)$ , and  $X(2500)$ .

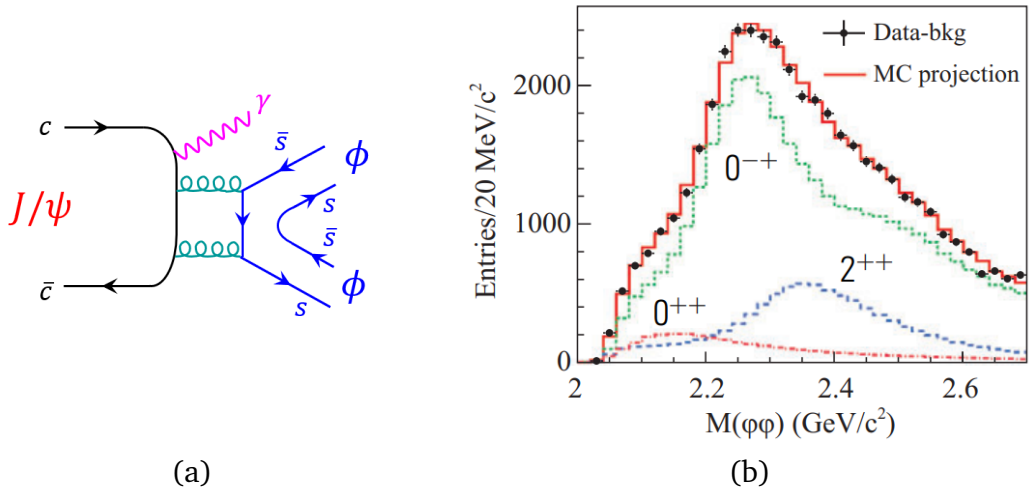


Figure 10: (a) Quark diagram for  $J/\psi \rightarrow \gamma \phi \phi$  radiative decay and (b) Intensities of individual  $J^{PC}$  component from the PWA fit to the BESIII data.

Additionally, the scalar state  $f_0(2100)$  and three tensor states, the  $f_2(2010)$ ,  $f_2(2300)$  and  $f_2(2340)$  were identified[24]. The apparent difference between hadronic production experiments and radiative  $J/\psi$  decays presents an interesting opportunity to further investigate the  $\phi \phi$  system.

### 3 Experiment

We propose to measure the  $\bar{p}p \rightarrow \phi\phi$  reaction at the K1.8BR beam line in the momentum range of 0.90 GeV/c to 1.15 GeV/c in 0.05 GeV/c increments. The Hyperon Spectrometer will be used to detect events involving three or four charged tracks emerging from a liquid hydrogen target. This experiment will follow the experiment E72 (Search for a new narrow  $\Lambda^*$  resonance near the  $\eta\Lambda$  threshold) that utilizes  $K^-$  beams near 0.75 GeV/c. The proposed experiment takes an advantage of stable operation of the HypTPC during the E72 beam time.

#### 3.1 Beamline

The K1.8BR beam line can provide high-intensity  $\bar{p}$  beams with energies up to 1.2 GeV/c[25]. One of the main benefits of using the K1.8BR beam line is that the  $\bar{p}$  beam fully exploits the excellent momentum resolution of the K1.8BR line, resulting in a center-of-mass energy resolution of 1 MeV. J-PARC K1.8BR beam line was able to deliver  $2 \times 10^5$   $\bar{p}$  per spill during the 5.2 s duration, which equates to a rate of 40 kHz during the 50 kW operation[26]. Given the current proton beam power of the main ring (MR) exceeding 80 kW, it is estimated that the  $\bar{p}$  beam intensity can be scaled to 64 kHz at 80 kW.

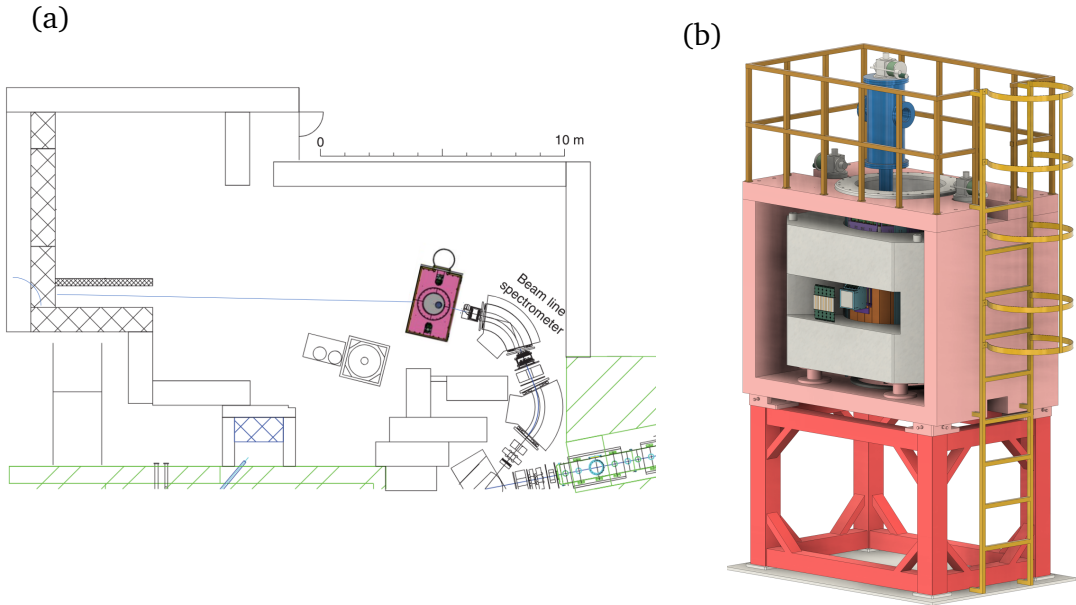


Figure 11: (a) The proposed location of the Hyperon Spectrometer at the K1.8BR beam line and (b) the Hyperon Spectrometer consisting of the HypTPC, LH<sub>2</sub> target, and HTOF.

Additionally, the background  $\pi^-$  beam intensity was roughly double that of the  $\bar{p}$  beam, resulting in a total beam intensity of 180 kHz or 720k/spill during the 4.24 s spill duration.

The experiment will start with a momentum of 0.90 GeV/c close to the  $\phi\phi$  threshold (0.866 GeV/c) and gradually increase to a maximum momentum of 1.15 GeV/c in 0.05 GeV/c increments. Consequently, the  $\bar{p}p \rightarrow \phi\phi$  reaction will be measured in 6 momentum bins.

### 3.2 Detector

We will be using the same setup as in the experiment E72, employing the Hyperon Spectrometer. After completing the E72 beam time, we can easily switch the  $K^-$  beam to  $\bar{p}$  beam by adjusting parameters of the K1.8BR beam line components. The beam aerogel counter (BAC) will reject any unwanted swift beam particles, such as  $\pi^-$ . Fast  $\pi^-$  beam particles always exhibit Cherenkov radiation, whereas slow  $\bar{p}$  beam particles do not radiate in the momentum range from 0.90 to 1.15 GeV/c. The BAC efficiency exceeds 99% with a 6-cm thick silica aerogel having a refractive index of 1.1.

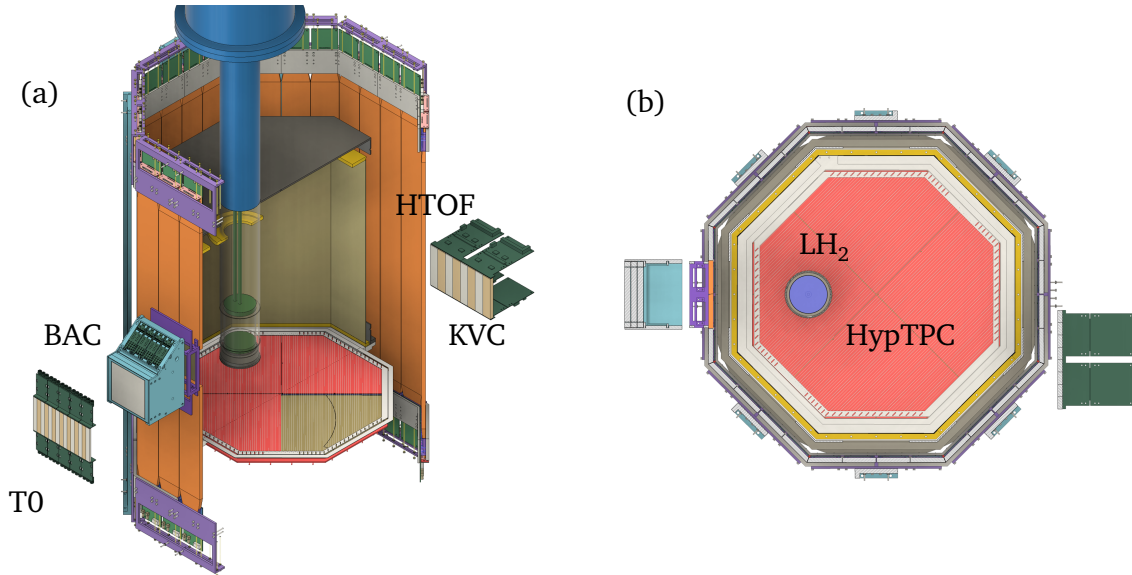


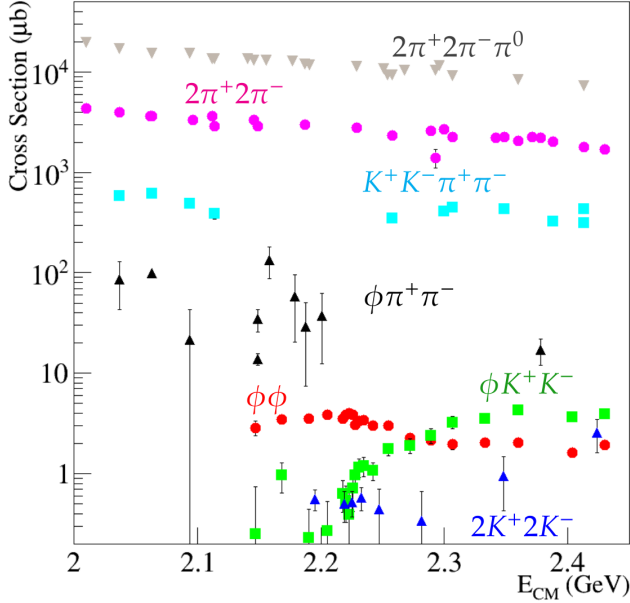
Figure 12: (a) Cross-sectional view of the Hyperon Spectrometer and (b) the plan view of the HypTPC and LH<sub>2</sub> target with surrounding detectors.

The beam will enter the HypTPC and may interact with a proton within a liquid hydrogen target located inside the HypTPC. The HypTPC serves as the primary tracker for this proposed experiment. The HypTPC has been successfully modified to incorporate a target holder. In addition, a new gas vessel has been installed, and ongoing cosmic-ray tests are conducted to optimize working parameters.

Four kaons from two  $\phi$  decays will create clear tracks that emerge from the target and reach the HTOF predominantly in the forward region.

### 3.3 Trigger Conditions

The online trigger focuses on efficiently reducing background processes involving reactions that produce multiple pions, such as  $\bar{p}p \rightarrow 2\pi^+2\pi^-\pi^0$ ,  $2\pi^+2\pi^-$ , and  $\pi^+\pi^-K^+K^-$ . The cross-section for  $\bar{p}p \rightarrow \phi\phi$  is much smaller than those for the background reactions by three orders of magnitude. Fig. 14 displays the total cross-sections for these processes in the momentum range of up to 2.5 GeV/c.



4-prong Reactions	$p_{\text{thre}}^{\text{lab}}$ (GeV/c)
$\bar{p}p \rightarrow 2\pi^+2\pi^-$	0
$\bar{p}p \rightarrow 2\pi^+2\pi^-\pi^0$	0
$\pi^+\pi^-K^+K^-$	0
$\pi^+\pi^-\phi$	0
$\bar{p}p \rightarrow 2K^+2K^-$	0.662
$\bar{p}p \rightarrow K^+K^-\phi$	0.767
$\bar{p}p \rightarrow \bar{p}p\pi^+\pi^-$	1.219
$\bar{p}p \rightarrow \bar{p}p\phi$	3.403

Table 2: Threshold momenta for background processes with four charged particle emission.

Figure 13: Total cross sections for the reactions  $\bar{p}p \rightarrow 4$  charged particles.

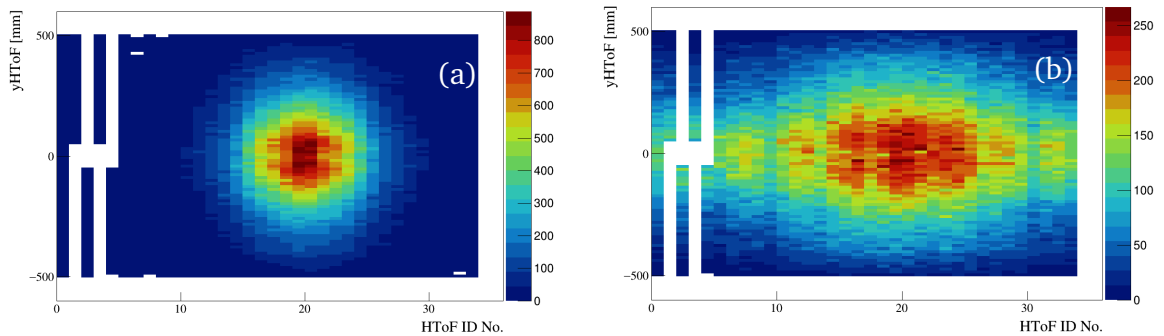


Figure 14: (a) HTOF hit patterns for  $\bar{p}p \rightarrow \phi\phi$  and (b) for  $\bar{p}p \rightarrow 2\pi^+2\pi^-$ . The HTOF encircles the HypTPC in 32 angular divisions. The forward  $0^\circ$ irc direction passes between the HTOF ID 19 and 20. Four short scintillators cover two backward angular divisions, creating a beam entrance.

The online trigger is characterized by the emission of four charged particles in the



forward direction for the  $\bar{p}p \rightarrow \phi\phi$  reaction. In particular, four kaons move forward near the threshold due to energy conservation, while lighter particles like pions can travel at large angles. Consequently, the trigger will necessitate at least three hits on the forward HTOF scintillators and no hit on the backward HTOF scintillators. The BAC will veto the  $\pi^-$  beam-induced background events and the KVC will not be part of the trigger.

This HTOF hit pattern constraint helps to significantly reduce background processes, while still detecting 92% of the  $\phi\phi$  events. The 5% inefficiency mainly arises from the in-flight decay of slow kaons. In the  $\phi \rightarrow K^+K^-$  decay, a typical momentum of  $K^+$  or  $K^-$  is 300 MeV/c in the  $\bar{p}p \rightarrow \phi\phi$  reaction at 1 GeV/c. The trigger efficiency is calculated using the E42 simulation software based on the Geant4 simulation toolkit with a full geometry of the Hyperon Spectrometer.

The trigger rates  $R$  are estimated using an expected intensity of  $\bar{p}$  beam of 64 kHz in the 80 kW operation, as shown in the following equation:

$$R(\text{Hz}) = 6.4 \times 10^4 / \text{s} \cdot N_p (\text{cm}^{-2}) \cdot (\sigma(\text{mb}) \times 10^{-27} \text{cm}^2) \cdot R_{\text{target}} \cdot \varepsilon_{\text{DAQ}} \cdot \varepsilon_{\text{trig}}.$$

This can be further simplified to:

$$R(\text{Hz}) \approx 1.5 \sigma(\text{mb}) \cdot \varepsilon_{\text{trig}}.$$

Here,  $N_p$  represents the number of target protons per unit area ( $\text{cm}^2$ ), which can be calculated as  $N_p = \rho(n_p N_A / M)L \approx 3 \times 10^{23} / \text{cm}^2$ . The density of LH<sub>2</sub> ( $\rho$ ) is  $7.085 \times 10^{-2} \text{ g/cm}^3$  and the number of protons in an H<sub>2</sub> molecule ( $n_p$ ) is 2. Avogadro's number is denoted by  $N_A$  ( $6 \times 10^{23} / \text{mol}$ ) and the atomic mass of H<sub>2</sub> is 2 g/mol. The effective length of the LH<sub>2</sub> target is estimated to be 7 cm, passing the target cell with a diameter of 8 cm, and the factor  $R_{\text{target}}$  is 0.88, representing the beam profile fraction crossing the target area. The DAQ efficiency  $\varepsilon_{\text{DAQ}}$  assumed to be 0.9. Therefore, the trigger rate can be approximated as  $1.5 \cdot \sigma(\text{mb}) \cdot \varepsilon_{\text{trig}}$ . Finally, for the  $\phi\phi$  reaction, the trigger rate is calculated to be 0.046 Hz with  $\sigma = 3 \mu\text{b}$  and 0.92% trigger efficiency.

Reactions	$\sigma_{\text{tot}}$ at 1 GeV/c	Trigger efficiency ( $\varepsilon_{\text{trig}}$ )	Expected trigger rate
$\bar{p}p \rightarrow 2\pi^+2\pi^-\pi^0$	15 mb	25%	50 Hz
$\bar{p}p \rightarrow 2\pi^+2\pi^-$	3.3 mb	20%	10 Hz
$\pi^+\pi^-K^+K^-$	0.5 mb	39%	4 Hz
$\bar{p}p \rightarrow \phi\phi$	3 $\mu\text{b}$	92%	0.046 Hz

Table 3: Expected trigger rates when requiring at least three HTOF hits in the forward region and no hit in the backward region.

Table 3 illustrates trigger efficiencies and expected trigger rates for the  $\phi\phi$  production and the dominant background processes. The total trigger rate would be less than 100 Hz or roughly 400/spill, allowing us to achieve a DAQ efficiency above 90%.



### 3.4 Detector Simulations

We performed a Monte Carlo simulation using the E42 simulation and analysis software for the  $\bar{p}p \rightarrow \phi\phi$  experiment. The event generator is based on the phase-space calculation for all possible channels involving the emission of four charged particles in  $\bar{p}p$  reactions. The total cross-section data are obtained from the compilation of  $\bar{p}$ -induced reactions [27]. In Fig. 15, simulated events for the  $\bar{p}p \rightarrow \phi\phi$  and  $\bar{p}p \rightarrow 2\pi^+2\pi^-$  reactions are displayed. Four tracks emerging from the LH<sub>2</sub> target are simulated using the HypTPC response of E42. The track simulation includes the actual non-uniform magnetic field map and the spatial resolution of the HypTPC.

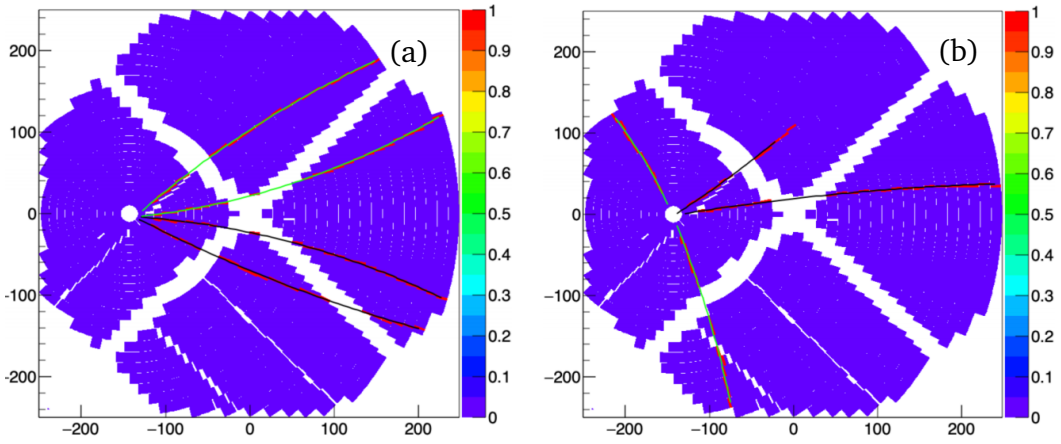


Figure 15: Simulated events for (a)  $\bar{p}p \rightarrow \phi\phi$  and (b)  $\bar{p}p \rightarrow 2\pi^+2\pi^-$  reactions. All charged tracks are assumed to share the same vertex at the target.

The event reconstruction follows the standard E42 offline analysis procedure. The track must contain a minimum of six TPC hits. Four tracks are searched for using the E42 track-finding algorithm based on the Hough transformation. Next, the tracks must share a single production vertex within the target region. The track momentum reconstruction starts with a helix fit to estimate initial track parameters, and implements the GENFIT tracking tool with the Runge-Kutta track extrapolation.

### 3.5 Event Selection

The HypTPC offers excellent separation capability between pions and kaons in the low momentum region. The 20% truncated mean values of energy loss ( $\langle dE/dx \rangle$ ) are plotted as a function of momentum/charge ( $p/z$ ) for reconstructed tracks in the diamond target dataset ( $C(K^-, K^+)X$  reactions) in Fig. 16. The energy-loss resolution ( $\sigma_{dE/dx}/\langle dE/dx \rangle$ ) is approximately 20% for the transverse momentum range  $0.40 < p_T < 0.45$  GeV/c.

This energy-loss information assists in identifying particles that meet the criteria for a  $K$ -like particle based on the particle identification function  $(dE/dx|_{\text{meas}} - dE/dx|_K)^2/\sigma_K^2$ . Fig.

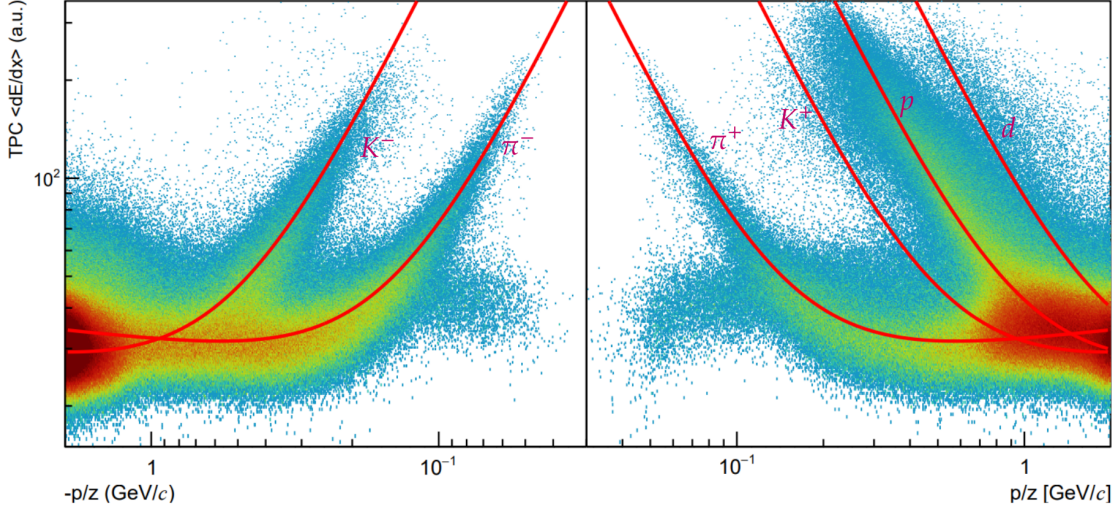


Figure 16: Specific energy loss  $\langle dE/dx \rangle$  vs. momentum/charge for tracks measured with the E42 HypTPC.

17(a) shows the simulated distribution of  $\langle dE/dx \rangle$  as a function of momentum/charge. Out of four tracks, events are chosen if at least three tracks were identified as kaons. This selection criteria reduces the reconstructed  $4\pi$  events to 6.8% and  $5\pi$  events to 1.2%. The  $5\pi$  events are then further rejected by requiring transverse momentum balance. It is possible for an undetected  $\pi^0$  to carry a significant amount of momentum in the transverse direction.

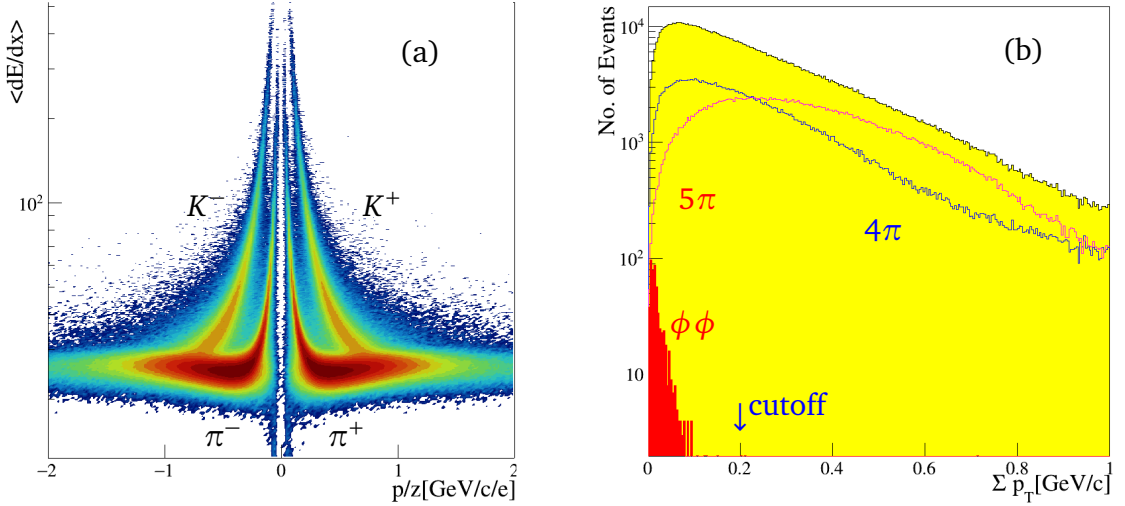


Figure 17: (a) Simulated  $\langle dE/dx \rangle$  vs  $p/z$  plot for  $\pi/K$  separation and (b) transverse momentum sum distributions.

In order to further select events, it is necessary to impose a balance constraint in the center-of-mass energy ( $\Delta m^2 = (p_{\bar{p}} + p_p)^2 - (\sum_{i=1}^4 p_i)^2 = 0$ , where  $p_i$  denotes a four-

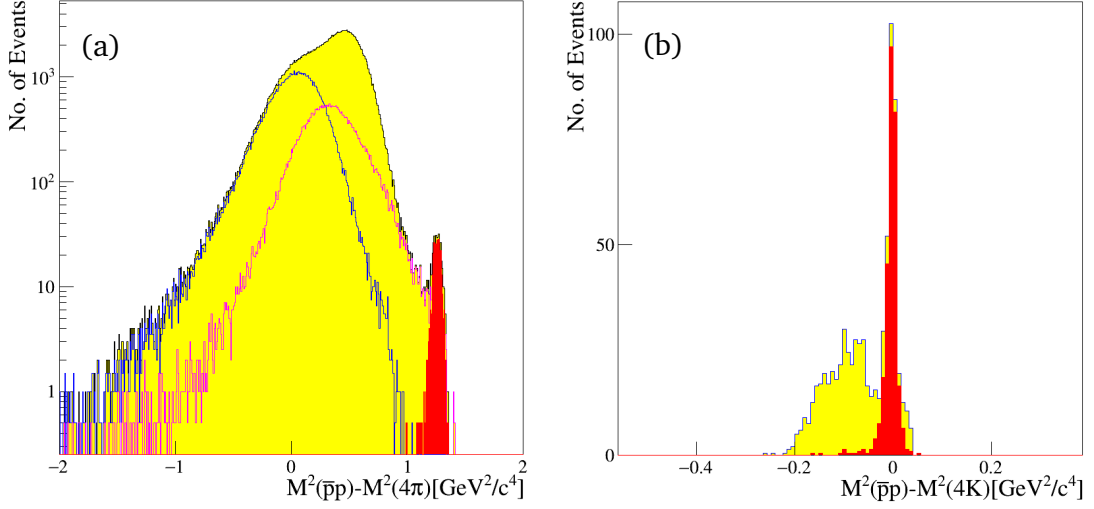


Figure 18: (a) Simulated distribution of  $\Delta m^2$ , the center-of-mass energy difference between the initial and final states assuming four pions are produced, and the  $\Delta m^2$  distribution for four  $K$  production after the  $\pi/K$  separation,  $p_T$  balance and  $\Delta m^2(4\pi)$  cutoffs are imposed.

momentum of particle  $i$ ) between the initial and final states. If we consider four kaon tracks, this energy balance requirement helps to distinguish the  $4K$  signal events from those involving background events with pions in the final state. When we assume that all particles are pions, the four kaon events are concentrated at the largest  $\Delta m^2$  value. The events above  $\Delta m^2 > 1 \text{ GeV}^2$  are selected in Fig. 18(a).

After imposing the  $4\pi$  balance cut, the four kaon events are selected by requiring that  $\Delta m^2 < 0.05 \text{ GeV}^2$ , as depicted in Fig. 18(b). The  $4K$  events are concentrated at  $\Delta m^2 = 0$ , while the other background events are spread across the negative region. When pions are produced at a specific center-of-mass energy of  $\bar{p}p$ , they may possess higher momentum than the more massive kaons. Assuming these pions are kaons, the center-of-mass energy of the final state should be higher than that of the initial state.

From two  $K^+$  and two  $K^-$  tracks, the correct pair of two oppositely charged kaons is chosen by selecting the pair with a mass closer to the nominal mass of the  $\phi$  meson. Background events involving pions are located on a parabolic curvature away from the  $\phi$  mass, as depicted in Fig. 19(a). Imposing all the event selection criteria, a strong accumulation of events can be observed at the nominal position of the  $\phi$  mass, as shown in Fig. 19(b).

### 3.6 $\phi$ Mass Resolution

In Fig. 19(b), the simulated  $K^+K^-$  mass distribution shows a mass resolution of 3 MeV considering the intrinsic width ( $\Gamma = 4.249 \text{ MeV}$ ) of the  $\phi$  meson. Analysis of E42 data

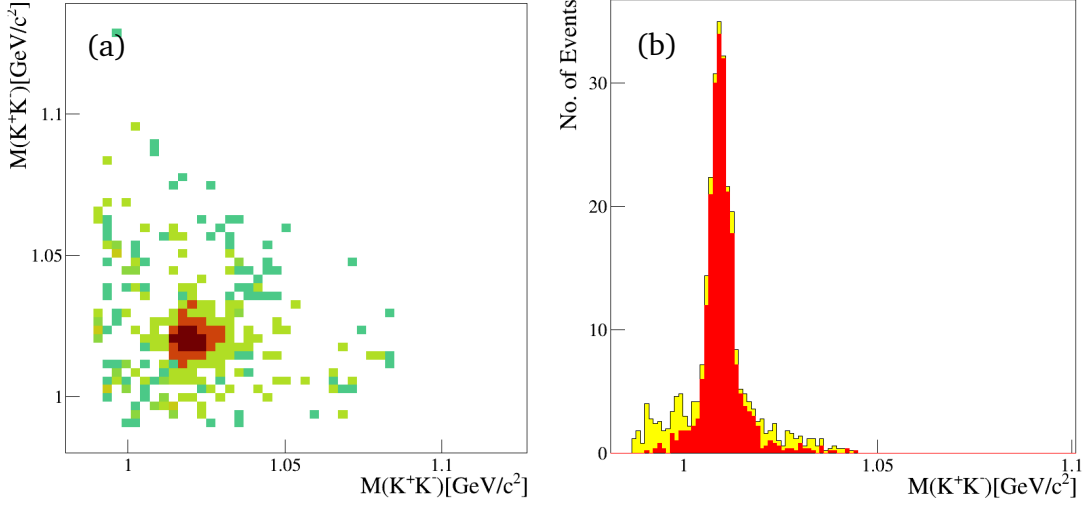


Figure 19: (a) Scatter plot of the simulated invariant masses of two  $K^+K^-$  pairs and (b) the  $K^+K^-$  invariant mass distribution when satisfying  $|m_{KK} - m_\phi| < 50 \text{ MeV}/c^2$ .

demonstrates the momentum resolution ( $\Delta p/p$ ) of the HypTPC ranges from 5% in the momentum range of 300 to 650 MeV/c to a minimum value of 3.4% at 400 MeV/c, crossing a 7% line at 800 MeV/c. A preliminary E42 analysis observes  $\phi$  production in the  $^{12}\text{C}(K^-, K^+)$  reaction at 1.8 GeV/c. The threshold momentum for the  $K^-p \rightarrow \Lambda\phi$  reaction is 1.763 GeV/c, which suggests that the  $\phi$  can barely be produced from  $K^-^{12}\text{C}$  reactions with a  $\Lambda$ . The  $\phi$  production is associated with a visible  $\Lambda$  decay, and the momentum distribution of the  $\phi$  is roughly 1.2 GeV/c, as shown in Fig. 20(a). The  $K^+K^-$  mass spectrum peaks at the nominal position of the  $\phi$  mass, with the mass resolution of 7 MeV, consistent with the momentum resolution.

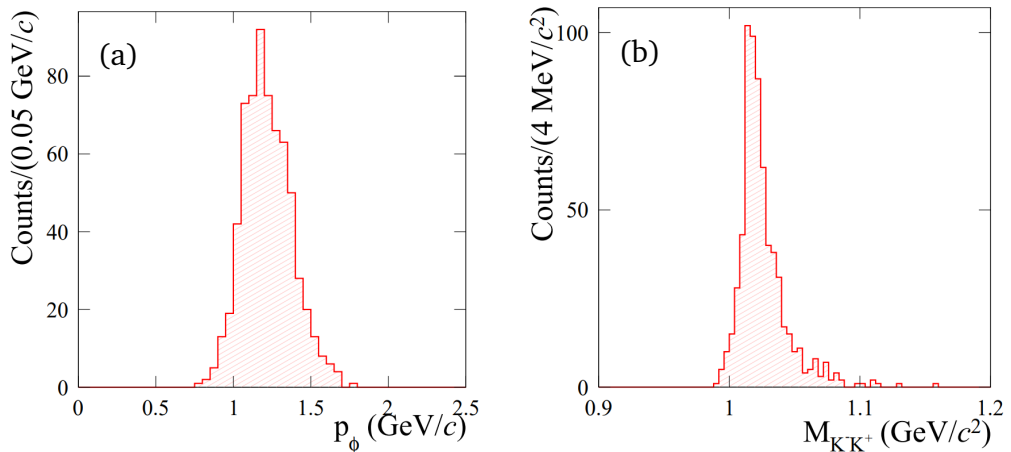


Figure 20: (a) Momentum distribution of reconstructed  $\phi$  events of the E42 data, and (b) the  $K^-K^+$  mass distribution.

### 3.7 Expected Yield of $\bar{p}p \rightarrow \phi\phi$ Events

For a beam intensity of  $6.4 \times 10^4$  Hz in the 80 kW MR operation the trigger rate for  $\phi\phi$  events is 0.046 Hz, as explained in the section on trigger conditions. Despite the online trigger system is capable of accepting a significant amount of background processes, primarily involving  $2\pi^+2\pi^-$  and  $2\pi^+2\pi^-\pi^0$  events, they are largely suppressed by imposing kinematic constraints and ensuring excellent  $\pi/K$  separation of the HypTPC. The reconstruction efficiency for the  $\phi\phi$  events is found to be 60%. Some of the rejected  $\phi\phi$  events are due to a  $\pi/K$  separation constraint for in-flight kaon decays. Additional offline analysis may save some of these events, but for a conservative estimate, the reconstruction efficiency is considered as  $\varepsilon_{\text{recon}} = 0.6$ .

Assuming the accelerator operates constantly 90% of the time ( $\varepsilon_{\text{acc}} = 0.9$ ), the number of  $\phi\phi$  events collected in a day is expected to be

$$N_{2\phi} = 0.046/\text{s} \cdot \varepsilon_{\text{acc}} \cdot \varepsilon_{\text{recon}} \cdot \text{Br}(\phi \rightarrow K^+K^-)^2 \cdot 8.64 \times 10^4 \text{ s/d} \approx 5.2 \times 10^2/\text{d},$$

where  $\text{Br}(\phi \rightarrow K^+K^-)$  denotes the branching ratio of the decay  $\phi \rightarrow K^+K^-$ , which is 0.491[28]. As a result, the expected yield for  $\phi\phi$  events ranges from approximately 200 to 500 events per day in the energy range from 2.05 ( $p_{\bar{p}} = 0.90$  GeV/c) to 2.13 GeV ( $p_{\bar{p}} = 1.15$  GeV/c). Fig. 21 represents the expected results on the total cross section measurement for the  $\bar{p}p \rightarrow \phi\phi$  reaction, assuming a high-statistics run at 1.15 GeV/c.

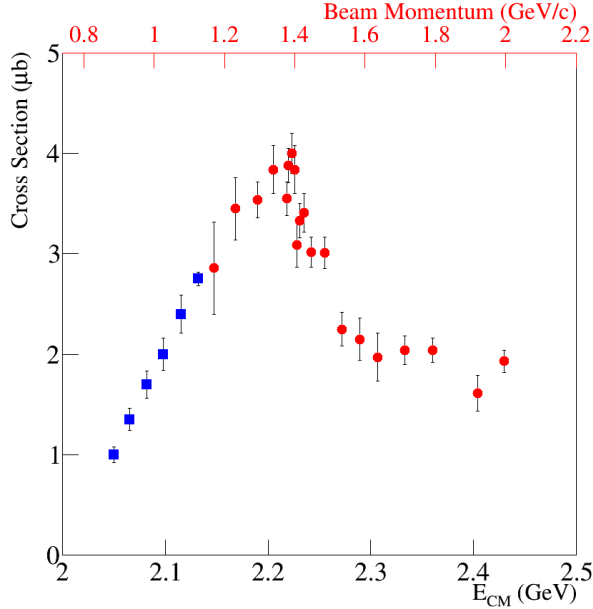


Figure 21: Expected results on the total cross-section measurement for the  $\bar{p}p \rightarrow \phi\phi$  reaction in the range of 0.90 to 1.15 GeV/c, overlated with the previous JETSET data.

## 4 Beam Time Request

We plan to conduct a measurement of the  $\bar{p}p \rightarrow \phi\phi$  reaction in the momentum range of 0.90 GeV to 1.15 GeV/ $c$ , with 0.05 GeV/ $c$  increments. This measurement will provide the first-ever data from the threshold to 1.10 GeV/ $c$ , and the data at 1.15 GeV/ $c$  will be compared with previous data from JETSET. As such, we need six days for data collection across six momentum settings, along with a half-day for trigger study. In summary, we are requesting 6.5 days of beam time. Out of the 6.5 days, three days will be dedicated to the high-statistics data collection at 1.15 GeV/ $c$  to measure polarization observables, with an expected order of 1500 events. The remaining three days will be allocated to measuring the  $\bar{p}p \rightarrow \phi\phi$  reaction at five momentum settings, allowing the statistical uncertainties in the total cross sections to be within the range of 5%-10%. It is worth noting that the JETSET experiment provides a value of  $(2.86 \pm 0.46)$  with 16% uncertainty at the lowest energy  $\sqrt{s} = 2.147$  GeV ( $p = 1.19$  GeV/ $c$ ).

## 5 Costs and Manpower

The operation cost of the Hyperon Spectrometer, as well as travel expenses and manpower, will be covered by current research grants from Korea, Japan, and the US. The manpower will include the HypTPC Collaboration and new members with particular expertise in exploring the  $\phi$  mesons in different reactions and utilizing a  $\bar{p}$  beam. The experts from K1.8BR will help in preparing this proposed experiment, which is crucial in assessing the beam line information.

## 6 Summary

We propose a new experiment to study double  $\phi$  production in  $\bar{p}p$  reactions in the momentum range of 0.90 ( $\sqrt{s} = 2.05$ ) to 1.15 GeV/ $c$  ( $\sqrt{s} = 2.13$  GeV) at the K1.8BR beam line. The cross section near the threshold, reported by the JETSET collaboration, shows an unusually high violation of the OZI rule in the  $\bar{p}p \rightarrow \phi\phi$  reaction. This violation, a few mb, is two orders of magnitude higher than the expected value of 10 nb from the SU(3) flavor mixing.

The proposed experiment will provide the first-ever data from threshold to 1.1 GeV/ $c$ , a region that has never been explored. The experiment aims to collect enough event statistics to measure the polarization observables in high momentum settings. These observables include spin density matrix elements and spin correlation variables.

A large acceptance of the HypTPC enables the measurement of the  $\bar{p}p \rightarrow \phi\phi$  reaction. This experiment should be conducted following the E72 during stable HypTPC operation. We are requesting 6.5 days of beam time, which includes half a day for the trigger study.

This experiment can be classified as a test experiment. It could also be a part of the experiment E29 (Searching for  $\phi$  meson bound state by H. Ohnishi), as the cross section of the elementary process  $\bar{p}p \rightarrow \phi\phi$  provides vital information for studying  $\phi N$  interaction in free space and a nuclear medium.

This experiment at J-PARC aims to advance the hadron physics program by using the HypTPC with an antiproton beam. The experiment will help explore the dynamics of gluons at low energies. The K1.8BR beam line will enable the production of vector-meson pairs near threshold, including  $\phi\phi$ ,  $\phi\omega$ , and  $K^*\bar{K}^*$ . By employing a deuterium target, the future experiment can search for a hidden-strangeness pentaquark state  $P_s$  through the reactions such as  $\bar{p}d \rightarrow \phi(\phi n)$  ( $p_{\text{th}} = 0.736$  GeV/ $c$ ),  $\phi(K^*\Sigma^0)$  ( $p_{\text{th}} = 1.042$  GeV/ $c$ ), and  $\phi(K^0\Sigma(1385)^0)$  ( $p_{\text{th}} = 0.516$  GeV/ $c$ ). The high-momentum beam from the K1.8 beam line covers a wide energy range up to 2.4 GeV ( $p = 1.91$  GeV/ $c$ ), allowing for the search of additional glueball candidates. A  $\bar{\Lambda}\Lambda$  cusp structure could appear near  $\sqrt{s} = 2m_\Lambda = 2.232$  GeV, being indicated by the sudden rise and fall in the cross sections. Additionally, the future experiment can investigate  $\bar{p}p \rightarrow \bar{\Lambda}\Lambda$  interactions, followed by  $\bar{\Lambda}p$  scattering.

## References

- [1] JETSET, *Il Nouvo Cimento* 107, 2329 (1994); JETSET, *Phys. Lett. B* 345, 325 (1995); JETSET, *Phys. Rev. D* 57, 5370 (1998).
- [2] H. Ohinishi, J-PARC E29, "Study of in medium mass modification for the  $\phi$  meson using  $\phi$  meson bound states in a nucleus" (2009).
- [3] F. Sakuma, J-PARC LoI, "Double anti-kaon production in nuclei by stopped anti-proton annihilation" (2009).
- [4] H.-W. Ke and X.-Q. Li, *Phys. Rev. D* 99, 036014 (2019).
- [5] Q.-F. Lü *et al.*, *Chinese Phys. C* 44, 024101 (2020).
- [6] Y. Chen *et al.*, *Phys. Rev. D* 73, 014516 (2006).
- [7] S. Narison, *Nucl. Phys. B*, 509, 312 (1998).
- [8] H.-X. Chen, W. Chen, and S.-L. Zhu, *Phys. Rev. D* 104, 094050 (2021).
- [9] J. Ellis *et al.*, *Phys. Lett. B* 353, 319 (1995).
- [10] N.I. Kochelev, *Phys.Atom.Nucl.* 59 (1996) 1643-1647, *Yad.Fiz.* 59N9, 1698 (1996).
- [11] Y. Lu, B.S. Zou, and M.P. Locher, *Z. Phys. A* 345, 295 (1994).
- [12] J. Shi, J.-P. Dai, and B.-S. Zou, *Phys. Rev. D* 84, 017502 (2011).
- [13] J.-J. Xie, L.-S. Geng and X.-R. Chen, *Phys. Rev. C* 90, 048201 (2014).
- [14] D.Y. Lee, J.K. Ahn and S.-i. Nam, to be submitted in *Phys. Rev. C* (2024).
- [15] K. P. Khemchandani, A. Martínez Torres, H. Nagahiro, and A. Hosaka *Phys. Rev. D* 88, 114016 (2013).
- [16] J. Davidson *et al.*, *Phys. Rev. D* 9, 77 (1974).
- [17] C. Baglin *et al.*, *Phys. Lett.* 231B, 557 (1989).
- [18] M. L. Vetere, *Nucl. Phys. B (Proc. Suppl.)* 56A, 256 (1997).
- [19] A. Etkin *et al.*, *Phys. Rev. Lett.* 41, 784 (1978).
- [20] A. Etkin *et al.*, *Phys. Rev. Lett.* 49, 1620 (1982).
- [21] A. Etkin *et al.*, *Phys. Lett. B* 165, 217 (1985).



- [22] A. Etkin *et al.*, Phys. Lett. B 201, 568 (1988).
- [23] Z. Bai *et al.*, Phys. Rev. Lett. 65, 1309 (1990).
- [24] BESIII, Phys. Rev D 93, 112011 (2016).
- [25] K. Agari *et al.*, Prog. Theor. Exp. Phys., 2012, 02B009 (2012); K. Agari, *et al.*, Prog. Theor. Exp. Phys. 2012, 02B011 (2012).
- [26] T. Hashimoto *et al.*, Beam profile measurement at K1.8BR, June 2023.
- [27] V. Flaminio, W.G. Moorhead, D.R.O. Morrison, and N. Rivoire, Compilation of cross-sections III :  $p$  and  $\bar{p}$  induced reactions, CERN-HERA 84-01, 17 April, 1984.
- [28] S. Navas *et al.* (Particle Data Group), to be published in Phys. Rev. D 110, 030001 (2024).